SUPPLEMENTAL MATERIAL

Sibling rivalry in *Myxococcus xanthus* is mediated by kin recognition and a polyploid prophage

Arup Dey, Christopher N. Vassallo, Austin C. Conklin, Darshankumar T. Pathak, Vera Troselj, and Daniel Wall

Department of Molecular Biology
University of Wyoming
1000 E. University Ave.
Laramie, WY 82071, U.S.A.

SUPPLEMENTAL TEXT

Sibling antagonism does not correlate to phenotypic differences in S-motility. We sought to investigate whether strain antagonism was correlated to phenotypic differences in motility between strains. To test this, we systematically assayed all possible combinations of motility phenotypes when strains were mixed and strain fitness was monitored by fluorescence microscopy. This method was chosen because it avoids technical problems associated with severe cell clumping of S-motile strains propagated on agar (unpublished results). First, we found that wild type (WT; A^+S^+) suffered a near 100-fold decrease in fitness when mixed with an A^-S^+ strain (Fig. S2A). Similarly, a >10-fold decrease in the WT fitness occurred when mixed with a nonmotile strain (A^-S^-). Although WT was outcompeted by both strains, the A^-S^+ strain reproducibly did so at a faster rate and to a larger degree (data not shown). In contrast, when WT was mixed with an A^+ S^-, strain there was no antagonism (Fig. S2A). Similarly, when both strains lacked A-motility (A^- S^- versus A^-S^+), there was no antagonism (Fig. S2B). However, similar to WT, the A^+ S^- strain was outcompeted by both the A^-S^+ and A^- S^- strains by nearly 100-fold (Fig. S2B). These antagonistic interactions were confirmed when an A^-S^+ strain was found to inhibit an A^+ S^- strain from swarming, which also was Tra dependent (Fig. S3). In summary, in these experiments, A-motile strains were antagonized by strains that lacked A-motility. In contrast, when both strains had identical A-motility phenotypes (A^- or A^+) they interacted harmoniously. These findings raised the possibility that phenotypic differences in A-motility led to killing.

***aglB1* is allelic to *aglQ* and does not cause antagonism**. The A-motility defects described in the above strains were all caused by the mutation *aglB1*. We sought to identify the gene associated with *aglB1* for two reasons: (i) the *aglB1* mutation was correlated with the kill phenotype, and (ii) the *aglB1* allele resides in DK1217, which is the parental strain used for the construction of DK1622 (1). DK1217 (A^-S^+) was made *aglB*$^+$ by phage transduction from the A-motile YS donor strain (see Fig. 5 for strain construction history). Because DK1217 and DK1622 are presumed isogenic strains and do not contain antibiotic markers, DK1217 was used by us and others as a reference A^-S^+ strain. To identify the *aglB1* mutation, the Tn*5*-Ω2213 insertion, which was 73% co-transducible with the *aglB* locus (data not shown), was sequenced. This insertion resides in MXAN_6867 and was therefore linked to the *aglRQS* operon (MXAN_6862/61/60) known to be involved in A-motility (2, 3). To test if the *aglB1* mutation was in *aglRQS,* the WT operon was cloned (pDP110) and found to rescue the A-motility defect of two *aglB1* strains (DK1217 and DK8601). This operon was sequenced from an *aglB1* mutant, and two mutations were found in *aglQ* (MXAN_6861). One mutation was silent and the other mutation was in codon 36 (TTC→ATC), resulting in a Phe→Ile substitution in a predicted transmembrane helix. Consistent with reports that AglQ functions as part of the A-motility motor (3), time-lapse microscopy studies found that *aglB1* mutants completely lacked single cell movements (data not shown). We conclude that *aglB1* is allelic to *aglQ* (F36→I) and this mutation abolishes A-motility.

To test whether phenotypic differences in A-motility caused by *aglB1* have a role in antagonism, this mutation was rescued in strain DK1217, yielding DW2401. This A^+S^+ strain was then mixed with a nonmotile aggressor (DK8601) and, importantly, no swarm inhibition was observed (Fig. S4A). In addition, DW2401 was mixed with a susceptible strain, and its ability to kill was identical to that of the DK1217 parental strain (Fig. S4B). In contrast, DK1622 did not antagonize the indicator strain. These results show that phenotypic differences in A-motility do not cause antagonistic interactions.

Table S1 Plasmids and primers used in this study

Plasmid/Primer	**Relevant properties**	**Source**
Plasmids		
pCR2.1-TOPO	Cloning vector, Km^r	Life Technologies
pCR-XL-TOPO	Cloning vector, Km^r Zm^r	Life Technologies
pAD3	*omrB* (insertion cassette) in pCR2.1 TOPO XL, Km^r Zm^r	(4)
pAD4	*traA* (insertion cassette) in pCR2.1 TOPO XL, Km^r Zm^r	This study
pCV101	ΔMx alpha cassette in pBJ114, Gal^s Km^r	This study (5)
pDP1	P_{pilA}-SS_{IM}-*mCherry* in pCR2.1 TOPO TA, Km^r	(6)
pDP2	*traA* (insertion cassette) in pCR2.1 TOPO TA, Km^r	(7)
pDP25	P_{pilA}-$traA^{M.fulvus}$ in pSWU19, Km^r	(8)
pDP110	*aglRQS* (*aglB*) in pCR2.1 TOPO TA, Km^r	This study
pTdTomato	P_{IPTG}-*td-Tomato* in pMR3487, Tc^r	Shimkets lab
pXW6	P_{pilA}-SS_{OM}-*mCherry* in pKSAT, Sm^r	(6)
Primers		
aglQRS FWD	ACGCGTCCTTCTTCACAAAC	This study
aglQRS REV	GACGTCAGGTCTGGAAGGTC	This study
Mx-alphaDelUp-F	AACAGCTATGACCATGATTACGCCAAGCTTCAGACCGAGCAGATCCCTAG	This study
Mx-alphaDelUp-R	ATCGCCGAGAACGCCAATAGCCCCAAGACTCCA	This study
Mx-alphaDelDn-F	TTGGGGCTATTGGCGTTCTCGGCGATTCTCTGA	This study
Mx-alphaDelDn-R	CGACGTTGTAAAACGACGGCCAGTGAATTCCCATCCTCTTCCGTCACCTT	This study
MXF1DRAFT_07228 FWD	GAGTCGATACCCACGCACT	This study
MXF1DRAFT_07228 REV	GAAGACGATGACTCCCGCTA	This study
traA KO FWD	TCACTGTCTTGTCGGTGTGC	(7)
traA KO REV	GCCGGTTGATGACCTGATAC	(7)

Table S2 Mx alpha polyploid units

		DZF1 Mx alpha paralogs; locus tag (DZF1DRAFT#); % amino acid identity	
DK1622 locus tags	**Predicted functions**	**Unit 1**	**Unit 2**
MXAN_1800	transposase, IS4 family	none	
MXAN_1801	RibD domain protein	none	07452; 96
MXAN_1802	hypothetical protein	07211; 90	07453; 84
MXAN_1803	hypothetical protein	none	
MXAN_1805	hypothetical protein	none	
MXAN_1806	hypothetical protein	none	
MXAN_1808	putative restriction/modification enzyme	none	
MXAN_1809	hypothetical protein	none	
MXAN_1810	RDD family protein	07206; 89	07459; 92
MXAN_1811	PBS lyase HEAT-like repeat protein	7205; 88	07460; 94
MXAN_1812	hypothetical protein	7202; 37	07463; 39
MXAN_1813	hypothetical protein	none	07464; 31
MXAN_1814	hypothetical protein	none	07465; 30
MXAN_1815	hypothetical protein	07199; 37	07466; 38
MXAN_1816	hypothetical protein	07198; 67	07467; 66
MXAN_1817	hypothetical protein	none	07468; 95
MXAN_1818	hypothetical protein	07197; 100	07469; 99
MXAN_1819	hypothetical protein	07196; 93	07470; 88
MXAN_1820	hypothetical protein	07195; 97	07471; 92
MXAN_1821	hypothetical protein	07193; 97	07473; 95
MXAN_1822[a]	hypothetical protein	07191; 44	none
MXAN_1823	hypothetical protein	none	
MXAN_1824[a]	hypothetical protein	07272; 38	07474; 95
MXAN_1826[a]	hypothetical protein	07273; 75	07192; 54
MXAN_1827	hypothetical protein	none	
MXAN_1828	hypothetical protein	none	
MXAN_1829	hypothetical protein	07271; 99	07190; 83
MXAN_1831	hypothetical protein	07270; 97	07189; 85
MXAN_1832	hypothetical protein	07268; 96	07188; 85
MXAN_1833	hypothetical protein	07267; 99	none
MXAN_1834	hypothetical protein	07266; 95	07187; 88
MXAN_1835	hypothetical protein	07265; 95	07186; 93
MXAN_1836	putative phage tail protein	07264; 94	07185; 93
MXAN_1837	hypothetical protein	07263; 92	07184; 95

MXAN_1838	hypothetical protein	07262; 97	07183; 96
MXAN_1839	hypothetical protein	07261; 90	07182; 87
MXAN_1840	hypothetical protein	07260; 96	07181; 96
MXAN_1841	hypothetical protein	07259; 78	07180; 77
MXAN_1842	hypothetical protein	07258; 90	07179; 88
MXAN_1843	hypothetical protein	07257; 94	07178; 92
MXAN_1844	hypothetical protein	07256; 96	07177; 95
MXAN_1845	putative phage late control gene D protein	07255; 99	07417; 94
MXAN_1846	hypothetical protein	07254; 98	07416; 89
MXAN_1847	hypothetical protein	07253; 95	07415; 95
MXAN_1848	phage tail tape measure protein, TP901 family	07251; 95	07414; 93
MXAN_1849	hypothetical protein	07250; 98	07413; 89
MXAN_1850	hypothetical protein	07249; 95	07412; 94
MXAN_1851	conserved hypothetical phage tail region protein	07248; 97	07411; 96
MXAN_1852	putative phage tail sheath protein	07247; 95[b]	07210; 93[b]
MXAN_1853	putative phage sheath protein	07247; 91[b]	07210; 89[b]
MXAN_1854	hypothetical protein	07246; 84	07409; 93
MXAN_1855	IPT/TIG domain protein	07245; 97	07408; 93
MXAN_1856	hypothetical protein	07244; 97	07407; 96
MXAN_1857	hypothetical protein	07243; 94	07406; 96
MXAN_1858	hypothetical protein	07242; 88	07405; 86
MXAN_1859	hypothetical protein	07241; 95	07404; 96
MXAN_1860	hypothetical protein	07240; 95	07403; 95
MXAN_1861	hypothetical protein	07239; 94	07402; 91
MXAN_1862	phage-like element pbsx protein xkdg	07237; 99	07401; 97
MXAN_1863	hypothetical protein	07236; 96	07399; 75
MXAN_1864	N6 adenine-specific DNA methyltransferase	07235; 96	07398; 95
MXAN_1865	hypothetical protein	07234; 89	07397; 84
MXAN_1866	putative phage head morphogenesis protein	07232; 92	07396; 93
MXAN_1867	hypothetical protein	07231; 95	07395; 91
MXAN_1868	phage portal protein, PBSX family	07230; 95	07394; 95
MXAN_1869	hypothetical protein	07226; 92	none
MXAN_1870	putative phage terminase, ATPase subunit	07627; 96	none

MXAN_1871	putative terminase, atpase subunit	none	
MXAN_1872	putative bacteriophage L54a, antirepressor	07633; 99	07625; 98
MXAN_1873	site-specific recombinase, phage integrase family	none	
MXAN_1874	hypothetical protein	07551, 89	07606, 93
MXAN_1875	hypothetical protein	07552; 89	07605; 94
MXAN_1876	exonuclease	07554; 97	07603; 95
MXAN_1877	hypothetical protein	07555; 95	07602; 93
MXAN_1878	hypothetical protein	07556; 88	07601; 85
MXAN_1879	hypothetical protein	07557; 68	07332; 94
MXAN_1880	hypothetical protein	07558; 86	07331; 86
MXAN_1881	hypothetical protein	07559; 95	07330; 91
MXAN_1882	putative helicase, ATP-dependent, intein-containing	07560; 81	07329; 90
MXAN_1883	hypothetical protein	07528 & 07561; 99[c]	07328; 94
MXAN_1884	hypothetical protein	07527; 88	07327; 99
MXAN_1885	putative bacteriophage related protein	07525; 92	07326; 95
MXAN_1886	hypothetical protein	07524; 88	07325; 81
MXAN_1887	site-specific recombinase, resolvase family	07523; 96	07324; 97
MXAN_1888	hypothetical protein	07522; 93	07323; 93
MXAN_1890	hypothetical protein	07521; 84	07322; 92
MXAN_1891	hypothetical protein	none	07321; 91
MXAN_1892	putative serine/threonine protein kinase	07519; 86	07320; 99
MXAN_1893	hypothetical protein	none	07319; 98
MXAN_1894	DNA-binding protein	07518; 87	07318; 99
MXAN_1895	DNA-binding protein	07517; 66	07317; 98
MXAN_1896	serine/threonine protein kinase	07516; 68	07316; 87
MXAN_1897	hypothetical protein	07515; 58	07315; 61
MXAN_1898	hypothetical protein	07514; 56	07314; 53
MXAN_1899	hypothetical protein	none	
MXAN_1900	hypothetical protein	07511; 68	07312; 70
MXAN_1901	transposase, IS5 family	none	

[a]paralogs

[b]fusion protein of MXAN_1852 and MXAN_1853

[c]two contigs that each partly cover MXAN_1883

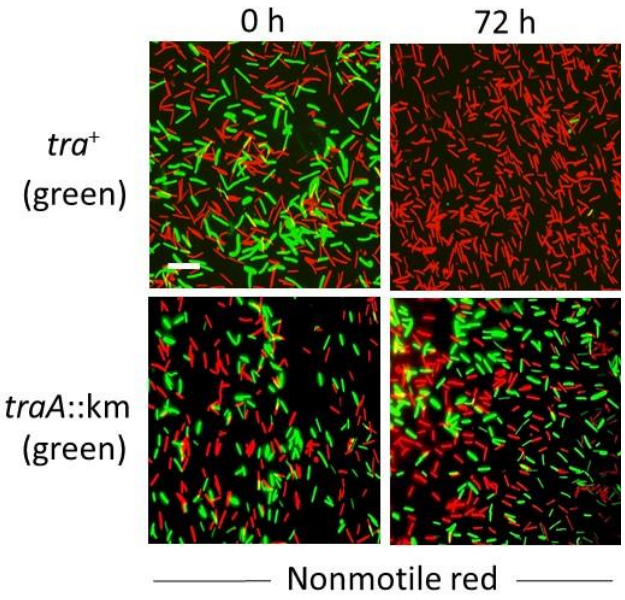

Fig. S1. Antagonism of A-motile cells by nonmotile cells is Tra-dependent. A nonmotile mCherry-labeled strain (DW1048) was mixed 1:1 with A-motile strains labeled with GFP that were either *tra*$^+$ (DW709) or *traA*::km (DW1613). At indicated times, cells were harvested and viewed on glass slides. Fluorescence micrographs were merged from the green and red channel. Bar, 10 µm.

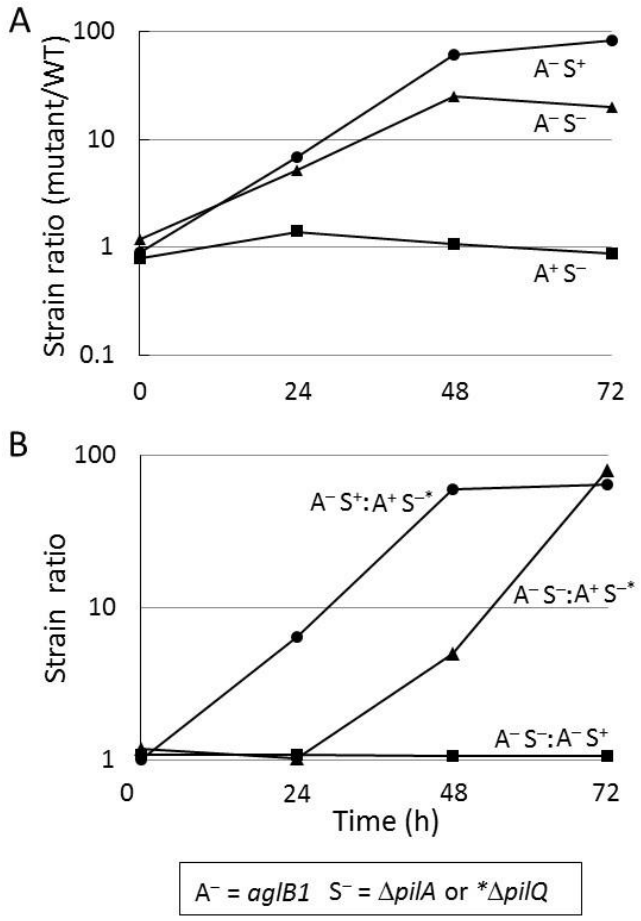

Fig. S2. A-motility mutants antagonize A-motile strains. A) An A^+S^+ strain labeled with mCherry (DW1616; WT) was mixed at a 1:1 ratio with three different types of motility mutants labeled with GFP (DW709, DK8605, and DK8606; phenotypes shown). The ratio of the strain mixtures was monitored over 72 h by harvesting cells from ¼ CTT agar plates and enumerating cell ratios by fluorescence microscopy. See Figure S1 for a representative panel image. B) All possible combinations of motility mutants were mixed and their fitness assessed as described in A. GFP-labeled strains were DK8605 and DK8606, and mCherry-labeled strains were DW1048 and DW1619. The *aglB1* allele was used for A-motility defects and all of these strains were derived from DK1217, whereas S-motility defects were caused by Δ*pilA* or Δ*pilQ* alleles and all strains were derived from DK1622. See Table 1 for strain details.

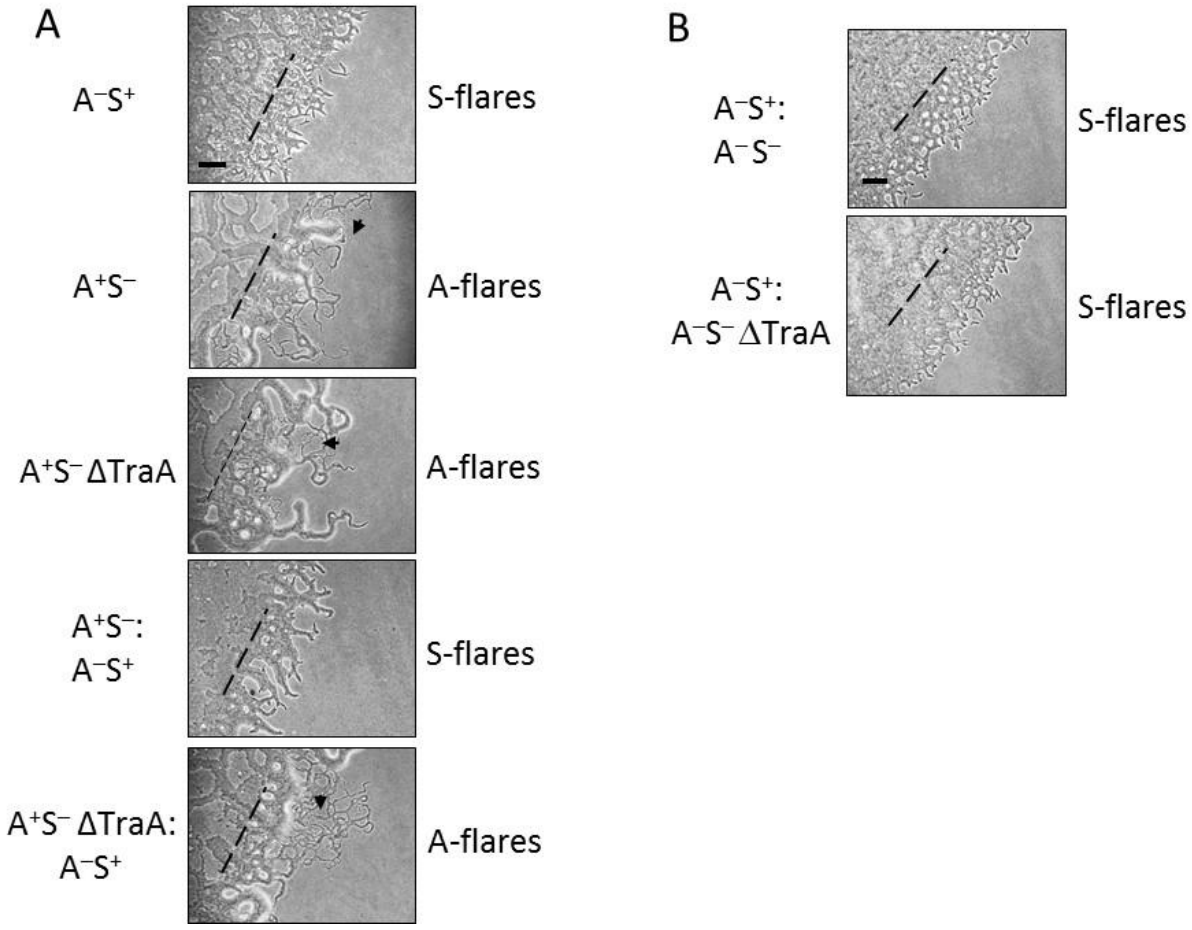

Fig. S3. Antagonism of A-motility by an $A^{-}S^{+}$ mutant. A) Aliquots of indicated monocultures or mixed cultures (1:1 ratio) were placed on TPM agar and incubated for 24 h. Arrows mark individual cells or small groups of cells (A-flares), which are characteristic of A-motility and were absent from the $A^{+}S^{-}$:$A^{-}S^{+}$ strain mixture (which instead had S-flares). B) S-motile cells were not inhibited by nonmotile cells. Strains with indicated phenotypes were mixed 1:1 on TPM agar and incubated for 24 h. Strains used: DK1217 ($A^{+}S^{-}$), DK8615 ($A^{-}S^{+}$), DW1482 ($A^{+}S^{-}$ Δ*traA*), DK8601 ($A^{-}S^{-}$), and DW1467 ($A^{-}S^{-}$ Δ*traA*). Dashed lines, initial inoculum edge; bars, 100 µm.

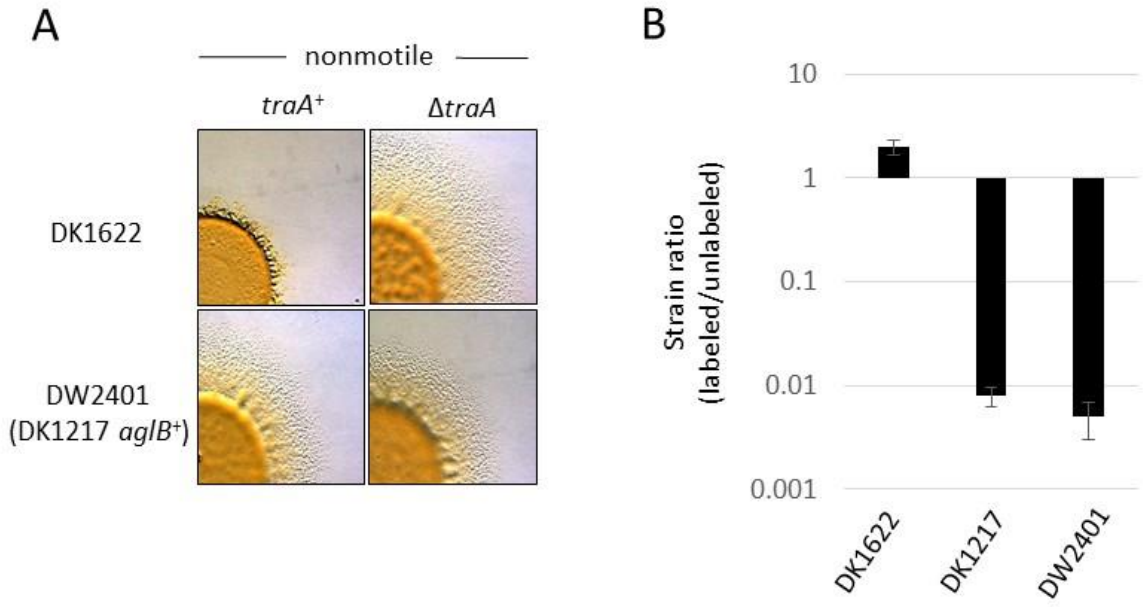

Fig. S4. The *aglB1* defect does not cause antagonism. A) Nonmotile strain DK8601 inhibits swarming of WT (A^+S^+; DK1622) by a Tra-dependent mechanism (Δ*traA*, DW1467). In contrast, an *aglB1* mutant (DK1217) rescued by an *aglB*$^+$ construct (A^+S^+; DW2401,) exhibits no inhibition. B) A susceptible strain that was labeled with mCherry (DW1619) was mixed 1:1 with a non-aggressor (DK1622) or a parental aggressor strain (DK1217) or DW2401. After 72 h, strain fitness was microscopically determined by counting labeled and unlabeled cells.

MOVIE LEGENDS

Movie S1. Time-lapse microscopy shows A-motile cells are inhibited from moving when mixed with nonmotile cells. Strains DK8615 and DK8601 were mixed 1:1 and visualized following a one day incubation on a ¼ CTT 1% agarose pad with 2 mM $CaCl_2$. Cells at the colony edge were viewed with a 20× phase contrast objective. Note, many of the cells at the swarm edge are not moving or are moving slowly. In two cases cells marked with arrows lyse. For a comparison see Move S2 where an isogenic Δ*traA* mutant was instead mixed. A 2-h movie was made with frames captured at 30-sec intervals. Movie format is MP4.

Movie S2. Time-lapse microscopy shows that a Δ*traA* mutant elicits wild-type A-motility when incubated with nonmotile cells. Strains DW1482 and DK8601 were mixed 1:1 and incubated as described in Movie S1 legend. A 1-h movie was made with frames captured at 30-sec intervals. Movie format is MP4.

REFERENCES

1. **Wall D, Kolenbrander PE, Kaiser D.** 1999. The *Myxococcus xanthus pilQ* (*sglA*) gene encodes a secretin homolog required for type IV pilus biogenesis, social motility, and development. J Bacteriol **181:**24-33.
2. **Youderian P, Burke N, White DJ, Hartzell PL.** 2003. Identification of genes required for adventurous gliding motility in *Myxococcus xanthus* with the transposable element mariner. Mol Microbiol **49:**555-570.
3. **Sun M, Wartel M, Cascales E, Shaevitz JW, Mignot T.** 2011. Motor-driven intracellular transport powers bacterial gliding motility. Proc Natl Acad Sci U S A **108:**7559-7564.
4. **Dey A, Wall D.** 2014. A genetic screen in *Myxococcus xanthus* identifies mutants that uncouple outer membrane exchange from a downstream cellular response. J Bacteriol **196:**4324-4332.
5. **Julien B, Kaiser AD, Garza A.** 2000. Spatial control of cell differentiation in *Myxococcus xanthus*. Proc Natl Acad Sci U S A **97:**9098-9103.
6. **Wei X, Pathak DT, Wall D.** 2011. Heterologous protein transfer within structured myxobacteria biofilms. Mol Microbiol **81:**315-326.
7. **Pathak DT, Wei X, Bucuvalas A, Haft DH, Gerloff DL, Wall D.** 2012. Cell contact-dependent outer membrane exchange in myxobacteria: Genetic determinants and mechanism. PLoS Genet **8:**e1002626.
8. **Pathak DT, Wei X, Dey A, Wall D.** 2013. Molecular recognition by a polymorphic cell surface receptor governs cooperative behaviors in bacteria. PLoS Genet **9:**e1003891.